Finite Element Analysis of the Interaction of Hydrogen Induced Stepwise Cracks

Cortés Suárez V.J.[(1)], González Velázquez J.L.[(2)], Hallen López J.M[(2)] and Reséndiz Robles J.G.[(2)]

Universidad Autónoma Metropolitana, Unidad Atzcapotzalco
Av. San Pablo No. 180, Col. Reynosa, México D.F. 02200

Instituto Politécnico Nacional, ESIQIE, Dep. Ing. Metalúrgica
Apdo. Postal 75-872, México, D.F. 07300
e-mail: gaid@prodigy.net.mx

Abstract.

The interaction between two near by hydrogen induced cracks was calculated considering their: length, distance between planes and crack tip separation. A superimposed uniform tensile stress and an interval of hydrogen pressure inside of the cracks were considered in the model. The interaction is reported in terms of the stress intensity factor in mode I and mode II, normalized with respect to the stress intensity factor of an isolated crack. Assuming that the crack propagates in a direction normal to the highest local normal stress in the crack tip, it was possible to predict the propagation trajectory of two interacting cracks.

1. Introduction.

The problem of the interaction of two near cracks can be found in a wide variety of cases[1], in particular, the hydrogen induced cracking (HIC) in steel pipelines that transport sour hydrocarbons is characterized by the formation of an array of stepwise cracks that may be interconnected. In sour environments, the hydrogen produced by the corrosion reaction diffuses through the steel and is collected in elongated manganese sulfide inclusions, forming hydrogen gas at very high pressures in those sites. The high hydrogen pressure forms an array of parallel cracks that may interconnect by the interaction of their crack tip stress fields and the hoop stress in the pressurized pipe[2-5]. The growth and coalescence of individual cracks can continue up to cause the pipeline fracture; that is why there have been several studies about the interaction and coalescence crack phenomena of HIC in steels[6-12]. In some of these studies, only the effect of the externally imposed stress was analyzed, while others consider the simultaneous effect of the hydrogen pressure inside the crack and an imposed uniform tensile stress[13-15], which magnitude is several orders of magnitude higher than the stress produced by the operation pressures actually used in sour hydrocarbon transport pipelines. With the purpose of analyzing the behavior of HIC cracks in more realistic conditions, in the present work, a finite element stress analysis (FESA) was done to determine the effect of the internal hydrogen pressure and uniform tensile stress on the interaction and coalescence of HIC

cracks. The analysis is limited to a two dimensional case and assuming that the material behaves as an isotropic, linear elastic solid.

2. Modeling and Experimentation.

The model consisted of two parallel cracks with internal pressure in the mid thickness section of an internally pressurized pipe. The stress field was then calculated by the finite element method. The pipe dimensions were 649 mm of external diameter and 12.7 mm of wall thickness, this because this is one of the most common pipe specification used for the transportation of sour gas in the oil industry. The pipe is under an internal pressure that produces a hoop stress so the internal crack experience that stress. Because there is not symmetry, it was necessary to model the complete array of the two neighboring cracks. The pipe curvature and longitudinal stress in the pipe were neglected and the final model consisted of a flat plate with two internal cracks with pressure inside and a superimposed uniform tensile stress, equivalent to the membrane stress due to the pipe pressure, acting parallel to the cracks. Figure 1 shows a drawing of the general model used here.

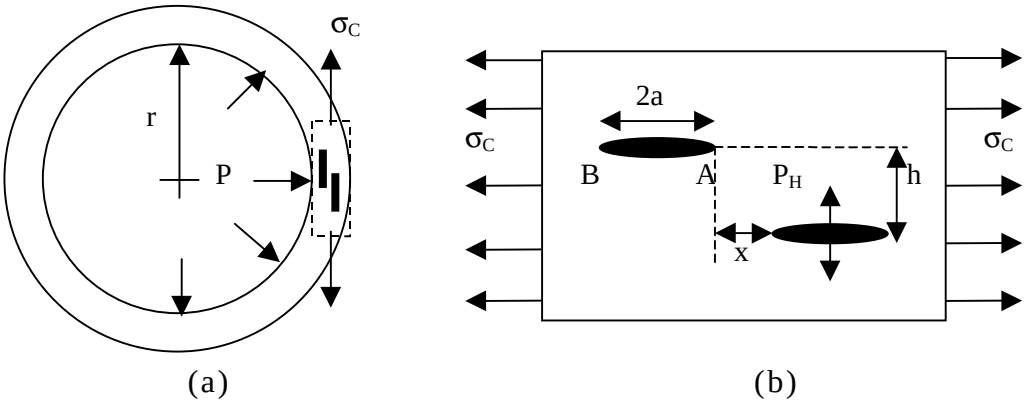

Fig. 1.- (a) Transversal view of a pipe showing the location of the HIC cracks; (b) Model of two parallel cracks with internal pressure and a uniform tensile stress. P = pipe internal pressure, σ_C = hoop stress, r = internal pipe radius, t = pipe wall thickness, P_H = crack internal pressure, 2a = crack length, x = horizontal crack tip separation, h = vertical crack separation, A = internal crack tip and B = external crack tip.

The plate was modeled in two dimensions, with a width of 25.4 mm, height of 12.7 mm and unitary thickness. The average crack length (2a) was 500 μm, separated in the horizontal direction (x) from 500 to 500 μm in 250 μm intervals and from 0 to 600 μm with intervals of 200 μm in the vertical direction (h). The applied stresses were 235, 176.4 and 117.6 MPa that correspond to a pipe internal pressure of 9.8, 735 and 4.9 MPa. The pressure inside the cracks were taken as 1000, 500, 250 and 100 MPa. The steel mechanical properties were those for an API 5L X52 pipeline steel and were: Young's modulus 205 GPa, Poisson's ratio 0.33 and yield strength 52 ksi. The finite element mesh

was a square with 8 nodes and 2 degrees of freedom in plane strain, this because the cracks are completely embedded in the plate. The crack tips closer to each other are referred as internal and the opposite or far crack tips are the external. The following quantities were calculated:

a) The Mode I stress intensity factor for an isolated crack (Ko)
b) The Mode I stress intensity factor for the internal crack tip (K_{IA}) and external crack tip (K_{IB}).
c) The Mode II stress intensity factor for the internal (K_{IIA}) and external (K_{IIB}) crack tip.

These values were used to find the crack propagation angle (θ_m). For an isolated crack the stress intensity factor (SIF) was calculated considering both the internal pressure in the crack (P_H) and the hoop stress (σ_C) as:

$$(P_H + \sigma_C)\sqrt{\pi a}\, f\left(\frac{a}{W}\right) = Ko \qquad (1)$$

The FESA program used to calculate the Mode I and Mode II SIF here, is based on the calculus of the displacements in the vicinity of the crack tip; the corresponding expressions are:

$$K_I = \sqrt{2\pi}\,\frac{G}{1+\chi}\,\frac{|\Delta u|}{\sqrt{r}} \qquad (2)$$

$$K_{II} = \sqrt{2\pi}\,\frac{G}{1+\chi}\,\frac{|\Delta v|}{\sqrt{r}} \qquad (3)$$

Where Δu and Δv are the displacements in the x and y directions respectively, G is the elastic shear modulus, $\chi = (3 - 4\nu)$ for plane strain, ν is the Poisson's ratio and r and θ are the polar coordinates from the crack tip.

The crack propagation angle was obtained from the maximum normal stress criterion proposed by Erdogan and Sih[16] that establishes that a crack will propagate in the direction normal to the maximum tensile stress (σ_θ), so σ_θ is the maximum principal stress. The angle θ is calculated from the expression for σ_θ:

$$\sigma_\theta = \frac{1}{\sqrt{2\pi r}}\cos\frac{\theta}{2}\left[K_I\cos^2\frac{\theta}{2} - \frac{3}{2}K_{II}\sin\theta\right] \qquad (4)$$

By taking the fist derivative $(\delta\sigma_\theta/\delta\theta) = 0$, σ_θ is a maximum, that is the principal stress, and solving for θ we get:

$$\theta_m = \pm \arccos\left[\frac{3K_{II}^2 + K_I\sqrt{8K_{II}^2 + K_I^2}}{K_I^2 + 9K_{II}^2}\right] \qquad (5)$$

The positive sign is taken when $K_{II} \leq 0$ and vice versa.

In addition to the FESA simulations, HIC experiments were conducted by cathodic charging plates made of API 5L X52 steels, according to the method proposed by Eiber and Bunenik[17]. By means of metallographic examination in both optical and scanning electron microscopy the different HIC crack configurations were recorded and the dimensions *2a, h, x* and θ were measured and compared with the model predictions to validate its results.

3. Results and Discussion.

3.1 Mode I Stress Intensity Factor.

Figure 2 shows the variation of K_{IA} and K_{IB} normalized with respect to Ko as a function of the horizontal (*x*) and vertical (*h*) separation of the crack tips. In these graphs it is observed that for both coplanar cracks (*h/2a=0*) and non coplanar cracks (*h/2a > 0)*, of K_{IA} and K_{IB} increase as the crack tips get closer, reaching a maximum when the crack tips are in an orthogonal position (*x/a = 0*). When the crack tips begin to overlap, K_{IA} drop sharply. For separated crack tips (*x/a*> 4), K_{IA} and K_{IB} approach to Ko.

Figure 3 compares the values of K_{IA} and K_{IB} for non coplanar cracks. When the crack tips are very far apart (*x* is large), K_{IA} is larger than K_{IB} up to the point of orthogonal overlap, then K_{IB} is larger than K_{IA}.

3.2 Mode II Stress Intensity Factor.

The behavior for the Mode II SIF for the A tips, as a function of *x* is shown in figure 4. A first observation is that in both coplanar and non coplanar cracks, K_{IIA} has smaller values than K_{IA}. For non coplanar cracks, K_{IIA} changes sign as the crack tips approximate and overlap, and reach a minimum in the location *x/a* = -1. After this point, K_{IIA} increases as the overlap increases. It is noted that also K_{IIA} increases as the distance *h* gets shorter, and for crack tips far apart, K_{IIA} approaches to zero.

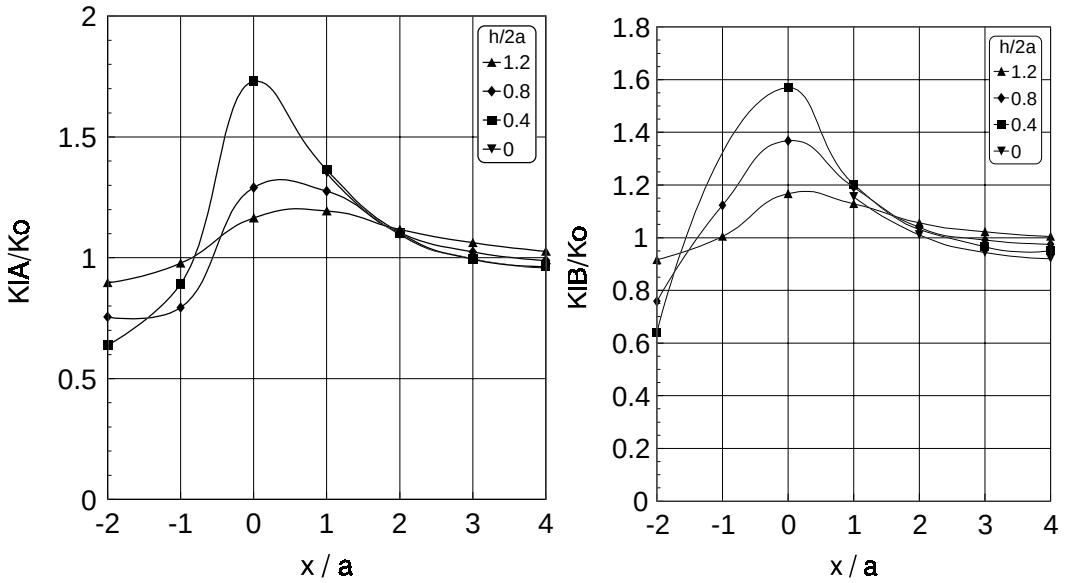

Fig. 2.- (a) Mode I SIF for internal crack tip K_{IA} and (b) Mode I SIF for the external crack tip K_{IB}. At P_H = 1000 MPa and σ_C = 235 MPa.

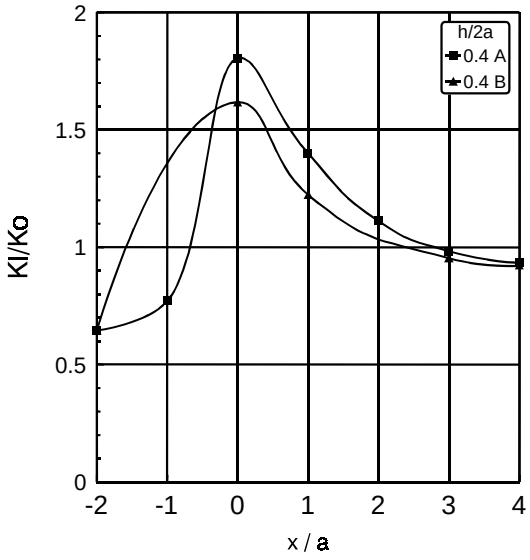

Fig. 3.- Normalized values of K_{IA} and K_{IB} for non coplanar cracks. P_H = 1000 MPa and σ_C = 235 MPa.

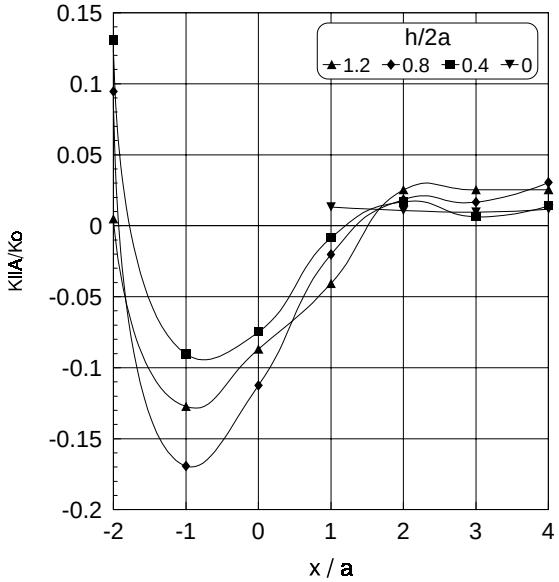

Fig. 4.- Variation of K_{IIA} for cracks with P_H = 500 MPa and σ_C = 174.6 MPa.

From the previous figures it is clear that as the crack tips get closer to each other and overlap, the Mode II is induced and K_{II} increases while the corresponding values of K_I are reduced due to the interaction. The same observation has been reported by Kitagawa[14] and indicates also that the overlapping crack tips should deflect as they approximate. The introduction of a Mode II in the SIF has other effects, as reported by Sih[15]: a) an increase in crack tip plasticity and b) the contact and fretting of opposite fracture surfaces, and both effects may reduce the crack growth rate. In a previous work regarding the kinetics of HIC[18], it was suggested that the interconnection of meeting cracks may reduce the crack growth rate, and this result may support that idea.

3.3 Crack Growth Direction.

The deflection angle of the internal crack tip A (θ_A) as a function of the crack separations *x* and *h* for a pair of close cracks with a P_H = 500 MPa and σ_C = 117.6 MPa is shown in figure 5. It is observed that the internal crack tips begin to deflect as the get closer and overlap. In the point *x/a* = -1, θ_A reaches its maximum. This value also increases for cracks closer in the vertical direction.

This description agrees with the one reported by Wang *et. al.*[19] that concludes that the combination of Mode I and Mode II induce a deflection in the crack path, due to the introduction of shear stresses and the change in the sign of K_{II}.

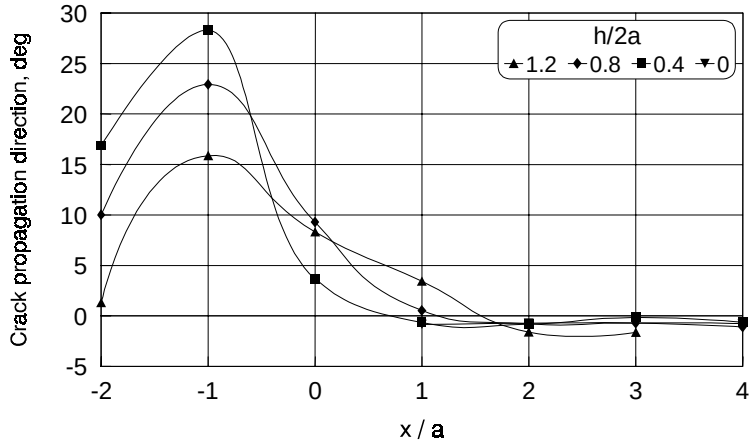

Fig. 5.- Deflection angle as a function of the crack tip separation for cracks with P_H = 500 MPa and σ_C = 117.6 MPa.

The figure 6(a) shows a pair of approaching HIC cracks with crack tip deflection produced in a cathodic charging experiment. The value of *x/a* is -0.2 and the vertical separation is *h/2a* = 0.43. The value of θ_A is 42 and 36 degrees for the upper and lower crack respectively. The calculated value is 5 deg. This great difference could be due to differences in P_H or in *2a*, simply because the cut may not be just at the center of the

cracks and the crack fronts may not be parallel. The figure 6(b) shows another pair of HIC cracks, generated in a plate with an applied stress. These cracks are closer than the ones in the figure 6 and it is clear that the deflection angle is greater in this case, in coincidence qualitatively with the predicted here

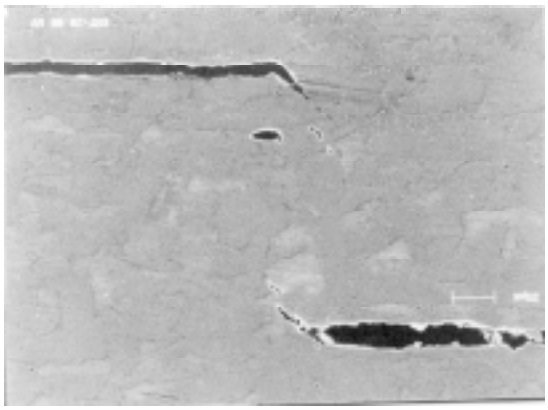

(a)

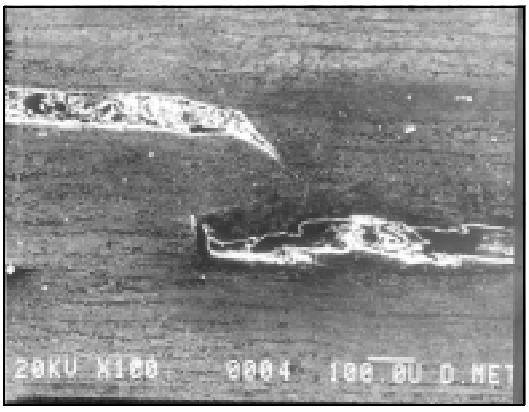

(b)

Fig. 6.- HIC cracks generated by cathodic charging (a) No stress applied, (b) with external stress applied

4. Conclusions.

1 The Mode I stress intensity factor for the crack tip of two neighboring cracks with internal pressure and superimposed tensile stress parallel to the cracks increases as the cracks approach to each other and diminishes as the cracks overlap.

2 The Mode II stress intensity factor is induced as the crack tips approach to each other and is maximum when the cracks overlap. Overlapping cracks experience a mix mode of growth which may reduce the crack growth rate.

3 Under a mix mode of growth, the crack tips of two approaching cracks with internal pressure deflect and tend to interconnect, with the deflection angle being larger as the cracks overlap and are closer in the vertical direction.

5. References.

1. J.F. Dwyer, Engineering Fracture Mechanics, Vol. 56, No. 2 (1997), pp. 233-248
2. R.D. Kane, Int. Metals Rev., Vol. 30 No. 6 (1985), pp. 291-301
3. M. Kimura, N. Totsuka, T. Kurisu, K. Amano, J. Matsuyama & Y. Nakai, Corrosion, Vol. 45 No. 4 (1989), pp. 340-346
4. G. Herbsleb, R.K. Poepperling & W. Schwenk, Corrosion, Vol. 36 No. 5 (1981), pp. 247-256
5. A. Brown & C.L. Jones, Corrosion , Vol. 40 No. 7 (1984), pp. 330-336
6. A. Kamei & T. Yokobori, Reports of the Research Institute for Strenght and Fracture of Materials, Vol. 20 No. 2 (1972), Tohoku University, Sendai, Japan
7. P.J.E. Forsyth, Int. J. Fatigue, Vol. 5 (1983), pp. 3-14
8. R.N. Parkins, E. Belhimer & W.K. Blanchard, Corrosion, Vol. 42 No. 12 (1993), pp. 951-966
9. Y.Z. Wang, D. Hardie & R.N. Parkins, Corrosion Science, (1994)
10. K.Y. Lam & S.P. Phua, Engineering Fracture Mechanics, Vol. 40 No. 3 (1991), pp 585-592
11. R.N. Parkins & P.M. Singh, Corrosion, Vol 46, No. 6 (1990), pp. 485-499
12. T. Yokobori, M. Uozumi & M. Ichikawa, Fract of Mats, Tohoku Univ., Vol. 7 (1971), p. 25
13. M. Iino, Met. Trans. A, Vol. 9A, (1978), pp. 1581-1590
14. H. Kitagawa, T. Fujita & M. Miyazawa, in Corrosion Fatigue Technology, Edited by H.L. Craig & D.W. Hoeppner, STP 624, pp. 98-114, Philadelphia, PA, ASTM
15. G.C. Sih, Int. J. Fract., Vol 10 (1974), pp. 305-320
16. F. Erdogan & G.C. Sih (1963) J. Basic Engng 85, 519-527
17. R.J. Eiber, T.A. Bunenik & W.A. Maxey, Fracture control technology for natural gas pipeline, Batelle Columbus Laboratories (1993)
18. J. L. González, R. Ramírez & J. M. Hallen, The Journal of Science and Engineering Corrosión, Vol. 53, No. 12 (1997), pp. 935-943
19. Y.Z. Wang, J.D. Atkinson, R. Akid & R.N. Parkins, Fatigue, Fract. Engng. Mater. Struct., Vol. 19 No. 4, (1996), pp 427-439

Acknowledgements.

The authors thank very deeply to the following institutions for their support for the development of this work: Instituto Politécnico Nacional, Pemex Exploración y Producción Región Sur and Universidad Autonoma Metropolitana. This work was financed by Pemex Exploración y Producción Región Sur, grant SRS GCTO 002/98.